Lateral Transcallosal Motor Fibers Reconstructed via Diffusion Tractography Do Not Reflect Homotopic Distributions

Longchuan Li[1], Matthew F, Glasser[2], Todd M Preuss[3], James K Rilling[3], Frederick W Damen[4], and Xiaoping Hu[1]

[1]School of Medicine, Emory University/Gerogia Institute of Technology, Atlanta, GA, United States, [2]Department of Anatomy and Neurobiology, Washington University, St Louis, MO, United States, [3]Center for Translational and Social Neuroscience, Emory University, Atlanta, GA, United States, [4]Department of Biomedical Engineering, Georgia Institute of Technology, Atlanta, GA, United States

Introduction: Studies in primates using tracing methods have shown that the primary motor cortex (M1) exhibits homotopic callosal projections, with the following characteristics: i) The strength of the callosal projection has a medial to lateral gradient, with dense connections found in M1 trunk and face representations, and sparse connections in M1 hand representation; ii) Each sector of M1 always has the densest callosal connection with the homotopic contralateral sector of M1(*1*, *2*). With the advent of diffusion MRI and tractography, it is well known that more lateral projections of the transcallosal fibers can now be mapped *in vivo* using sophisticated fiber-tracking algorithms that either can model crossing fibers or use a larger field of view (*3*, *4*). Here we go one step further to investigate whether the two above-mentioned characteristics of callosal projections can be quantitatively replicated using two advanced fiber-tracking algorithms, namely, global tractography (GT) (*4*)and local tractography (PT) (*3*), in humans.

Methods: Twenty young adults (10 females, 20±0.99 yrs) participated in this study. MRI images were obtained using a 3T Trio scanner (Siemens Trio, Malven, Pennsylvania, USA). T1-weighted images were acquired with a 3D MPRAGE sequence with the following parameters: FOV=256×256×176 mm^3, matrix size: 256×256×176, 1 mm isotropic voxels. Diffusion MR data were acquired with the following parameters: dual spin-echo diffusion echo-planar imaging sequence with GRAPPA (factor of 2), FOV=256×256 mm, matrix size=128×128, 64 slices covering the whole brain, 2 mm isotropic voxels, 64 directions, two averages with opposite phase encoding directions to remove the susceptibility distortion(*5*). Precentral gyral masks on the MNI152 template were first drawn manually and then evenly divided into four segments along the superior-inferior axis. Subsequently, these eight sectors were transformed into each individual's space and multiplied with the subject-specific gray-matter/white-matter (GMWM) interface mask to obtain an interface mask of the precentral gyrus. The interface masks for each sector were then used as seed masks and the connections between the eight seed masks were derived using GT and PT (M3 in (*6*)) and statistically compared. For GT, the count of streamline numbers was used as the index for connectivity strength. For PT, the thresholded tract volume was chosen as the index for connectivity strength(*6*).

Results: For both GT and PT, the strength of the transcallosal connections of the four homotopic sectors were significantly different (GT: $F_{(3,76)}$=53.26, p<10e-15; PT: $F_{(3,76)}$=23.25, p<8e-11), with the connection of L4-R4 significantly stronger than the other three homotopic sectors (p<0.05, Tukey-Kramer correction), largely consistent with the results of primate tracer studies (Fig.1). We then tested whether each sector of the precentral gyrus always has the densest transcallosal connection with corresponding contralateral homotopic sector (Fig.1). Results in both GT and PT demonstrated that only the homotopic sector pair of L4-R4 has the strongest transcallosal connection compared to their heterotopic pairs (i.e., L4-R3, L3-R4), suggesting that the transcallosal connections of the other sectors in the precentral gyri may not be quantitatively reflective of the findings in primate tracer studies. Similar results were also observed in data from two high-resolution post-mortem macaques, although the sample size is too small for statistical comparisons.

Discussions: Even though several recently developed tractography algorithms reported promising results in tracing lateral projections of the callosal fibers, it is possible that fibers from more lateral sectors of M1 may tend to erroneously terminate in more medial M1 sectors. Our results demonstrated that although GT and PT can trace more lateral projections of the transcallosal fibers, the strength of these transcallosal motor projections does not quantitatively reflect a homotopic distribution. The possible causes could be (i) bias of the tractography algorithms toward medial callosal fibers that do not intersect with other fiber systems, (ii) much weaker homotopic transcallosal connections in more lateral sectors compared to the medial sectors, making tractography results unreliable; (iii) sharper angles that need to be traversed for the lateral connections vs. the medial ones.

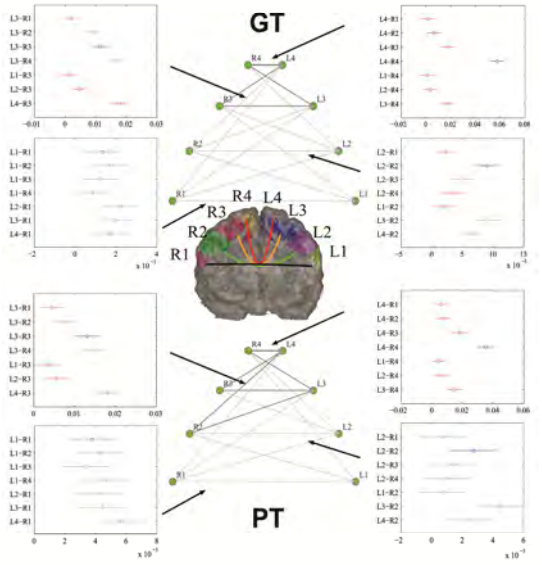

Fig.1. The networks of transcallosal fibers connecting two precentral gyri derived using GT and PT. For both GT and PT cases, the network topology is shown in the middle, with lines representing the connection strength. The four plots around each network topology indicate the statistical results (P<0.05, Tukey-Kramer correction). The connection strength between two edges (R-L) is significantly different if their confidence intervals do not overlap. Blue circles in the plots indicate homotopic sector pairs as pointed by the arrows. Red circles represent statistically significant differences compared to the blue ones.

Acknowledgement: This work was kindly supported by NIH 5P01 AG026423-03, R01 MH084068-01A1

References:

1. E. M. Rouiller *et al.*, *Exp Brain Res* **102**, 227 (1994).
2. P. C. Fang, I. Stepniewska, J. H. Kaas, *J Comp Neurol* **508**, 565 (Jun 1, 2008).
3. T. E. Behrens, H. J. Berg, S. Jbabdi, M. F. Rushworth, M. W. Woolrich, *Neuroimage* **34**, 144 (Jan 1, 2007).
4. M. Reisert *et al.*, *Neuroimage* **54**, 955 (Jan 15, 2011).
5. J. L. Andersson, S. Skare, J. Ashburner, *Neuroimage* **20**, 870 (Oct, 2003).
6. L. Li, J. K. Rilling, T. M. Preuss, M. F. Glasser, X. Hu, *Hum Brain Mapp* **DOI: 10.1002/hbm.21332**, (2011, 2011).